

# Accelerating rates of cognitive decline and imaging markers associated with $\beta$ -amyloid pathology

Philip S. Insel, MS  
Niklas Mattsson, MD,  
PhD  
R. Scott Mackin, PhD  
Michael Schöll, PhD  
Rachel L. Nosheny, PhD  
Duygu Tosun, PhD  
Michael C. Donohue,  
PhD  
Paul S. Aisen, MD  
William J. Jagust, MD  
Michael W. Weiner, MD  
For the Alzheimer's  
Disease Neuroimaging  
Initiative

Correspondence to  
P. Insel:  
philipinsel@gmail.com

## ABSTRACT

**Objective:** To estimate points along the spectrum of  $\beta$ -amyloid pathology at which rates of change of several measures of neuronal injury and cognitive decline begin to accelerate.

**Methods:** In 460 patients with mild cognitive impairment (MCI), we estimated the points at which rates of florbetapir PET, fluorodeoxyglucose (FDG) PET, MRI, and cognitive and functional decline begin to accelerate with respect to baseline CSF  $A\beta_{42}$ . Points of initial acceleration in rates of decline were estimated using mixed-effects regression.

**Results:** Rates of neuronal injury and cognitive and even functional decline accelerate substantially before the conventional threshold for amyloid positivity, with rates of florbetapir PET and FDG PET accelerating early. Temporal lobe atrophy rates also accelerate prior to the threshold, but not before the acceleration of cognitive and functional decline.

**Conclusions:** A considerable proportion of patients with MCI would not meet inclusion criteria for a trial using the current threshold for amyloid positivity, even though on average, they are experiencing cognitive/functional decline associated with prethreshold levels of CSF  $A\beta_{42}$ . Future trials in early Alzheimer disease might consider revising the criteria regarding  $\beta$ -amyloid thresholds to include the range of amyloid associated with the first signs of accelerating rates of decline.

**Neurology**® 2016;86:1887-1896

## GLOSSARY

**AD** = Alzheimer disease; **ADAS** = Alzheimer's Disease Assessment Scale; **ADNI** = Alzheimer's Disease Neuroimaging Initiative; **dRAVLT** = delayed Rey Auditory Verbal Learning Test; **FDG** =  $^{18}\text{F}$ -fluorodeoxyglucose; **MCI** = mild cognitive impairment; **OR** = odds ratio; **ROI** = region of interest.

Understanding the sequence of pathophysiologic processes occurring during the progression of Alzheimer disease (AD) has been a primary goal of recent research. Evidence has accumulated pointing to  $\beta$ -amyloid deposition and hypometabolism occurring in early stages with subsequent gray matter atrophy and cognitive and functional decline.<sup>1-3</sup> Hypothetical models have been proposed, though the details remain unclear.<sup>4</sup>

Understanding the timeframe of decline is required to facilitate targeting a specific process in order to slow progression.<sup>5</sup> Possible reasons for recent failures of clinical trials of anti-amyloid therapies include (1) targeting amyloid in patients who already exhibit substantial neurodegeneration and cognitive impairment and (2) failing to exclude patients without significant amyloid deposition.<sup>6-8</sup> Given these concerns, several current trials target  $\beta$ -amyloid pathology in earlier stages of the disease and require significant  $\beta$ -amyloid pathology.<sup>9</sup>

## Supplemental data at Neurology.org

From the Center for Imaging of Neurodegenerative Diseases (P.S.I., R.S.M., R.L.N., D.T., M.W.W.), Department of Veterans Affairs Medical Center, San Francisco; Departments of Radiology and Biomedical Imaging (P.S.I., D.T., M.W.W.) and Psychiatry (R.S.M.), University of California, San Francisco; Clinical Memory Research Unit, Faculty of Medicine (P.S.I., N.M.), Lund University; Memory Clinic (N.M.) and Department of Neurology (N.M.), Skåne University Hospital, Lund University; MedTech West and the Department of Clinical Neuroscience and Rehabilitation (M.S.), University of Gothenburg, Sweden; Department of Neurology (M.C.D., P.S.A.), Keck School of Medicine, University of Southern California, Los Angeles; Helen Wills Neuroscience Institute (W.J.J.), University of California, Berkeley; and Life Sciences Division (M.S., W.J.J.), Lawrence Berkeley National Laboratory, Berkeley CA.

Coinvestigators are listed on the *Neurology*® Web site at Neurology.org.

Data used in preparation of this article were obtained from the Alzheimer's Disease Neuroimaging Initiative (ADNI) database (adni.loni.usc.edu). As such, the investigators within the ADNI contributed to the design and implementation of ADNI and/or provided data but did not participate in analysis or writing of this report. A complete listing of ADNI investigators can be found at [https://adni.loni.usc.edu/wp-content/uploads/how\\_to\\_apply/ADNI\\_Acknowledgement\\_List.pdf](https://adni.loni.usc.edu/wp-content/uploads/how_to_apply/ADNI_Acknowledgement_List.pdf).

Go to Neurology.org for full disclosures. Funding information and disclosures deemed relevant by the authors, if any, are provided at the end of the article.

Amyloid positivity thresholds are frequently defined to be the level of pathology that most accurately distinguishes cases of AD from cognitively normal controls.<sup>10–12</sup> A recent report suggests that current Pittsburgh compound B thresholds are too high.<sup>13</sup> With more exclusive thresholds, it is likely that certain pathophysiologic processes have advanced beyond what is optimal for clinical trials intending to recruit participants with little neurodegeneration or cognitive impairment. Several measures of neurodegeneration have been shown to occur years prior to established  $\beta$ -amyloid thresholds.<sup>14–16</sup>

A priori thresholds, commonly used to study the effect of amyloid on neurodegeneration or cognition, preclude the detection of the initial acceleration of decline with respect to the level of  $\beta$ -amyloid. The goal of this study was to estimate the points along the spectrum of  $\beta$ -amyloid pathology at which rates of neuronal injury and cognitive decline begin to accelerate.

**METHODS Standard protocol approvals, registrations, and patient consents.** This study was approved by the institutional review boards of all of the participating institutions. Informed written consent was obtained from all participants at each site.

**Participants.** Data were obtained from the Alzheimer's Disease Neuroimaging Initiative (ADNI) database ([adni.loni.usc.edu](http://adni.loni.usc.edu), [www.adni-info.org](http://www.adni-info.org)). All sites had institutional review board approval to study human subjects. The population in this study included ADNI-2 participants enrolled into the mild cognitive impairment (MCI) cohort at screening, tested for CSF biomarkers, and followed longitudinally for at least one MRI, <sup>18</sup>F-fluorodeoxyglucose (FDG) PET, <sup>18</sup>F-florbetapir PET, or neuropsychological examination.

**CSF biomarker concentrations.** CSF samples were collected at baseline by lumbar puncture. CSF methods have been described previously.<sup>10,17</sup>

**MRI acquisition and processing.** Structural MRI brain scans were acquired using 3T MRI scanners with a standardized protocol.<sup>18</sup> Quantification was performed in an automated pipeline using FreeSurfer software package version 5.1 (<http://surfer.nmr.mgh.harvard.edu/fswiki>).<sup>19</sup> Detailed descriptions can be found at [www.adni-info.org](http://www.adni-info.org).

Regions of interest (ROIs) including the cingulate gyrus as well as the temporal, parietal, frontal, and occipital lobes were analyzed. Details about FreeSurfer parcellation can be found at <https://surfer.nmr.mgh.harvard.edu/fswiki/CorticalParcellation>. Left and right hemisphere volumes were averaged for each subregion.

**FDG PET.** Methods to acquire and process FDG PET images were described previously. Full details of procedures and the standardized protocol are described at <http://adni.loni.usc.edu/qw/methods/pet-analysis/pre-processing/and> at <http://www.adni-info.org/Scientists/ADNIStudyProcedures.html>. ROIs included in the analysis were the temporal, angular, and cingulate gyri.<sup>20,21</sup>

org/Scientists/ADNIStudyProcedures.html. ROIs included in the analysis were the temporal, angular, and cingulate gyri.<sup>20,21</sup>

**Florbetapir PET.** Similarly, methods to acquire and process ADNI florbetapir PET image data were described previously. Full details of acquisition and analysis can be found at <http://adni.loni.usc.edu/methods/>. ROIs included in the analysis were the temporal, parietal, and frontal lobes.<sup>11</sup>

**Cognitive and functional outcomes.** Cognitive measures assessed included the Mini-Mental State Examination, Alzheimer's Disease Assessment Scale–cognitive subscale, both the 11- and 13-item versions (ADAS-11, ADAS-13), delayed memory recall from the Wechsler Memory Scale (Logical Memory II), delayed Rey Auditory Verbal Learning Test (dRAVLT), Trail Making Test parts A and B, Boston Naming Test, a cognitive composite (comprising the ADAS-11, Logical Memory II, and the Trail Making Test part B), Clinical Dementia Rating Sum of Boxes, and the Functional Assessment Questionnaire.<sup>22–29</sup>

**Statistical analysis.** The relationship between longitudinal cognitive or imaging responses and baseline  $\beta$ -amyloid pathology was modeled in 2 steps. First, patient-specific rates for each response were estimated using all available data. Rates for responses with 3 or more observations per patient (cognition and MRI) were estimated using linear mixed effects regression with a random intercept and slope. Mixed effects models allow the number of responses to vary across individuals, adjusting for missingness. Longitudinal cognitive scores were regressed on time (years) since initial visit while adjusting for age, sex, and education. Volumes were regressed on time since initial visit while adjusting for age, sex, and intracranial volume. Rates for responses with only 2 observations per patient (FDG and florbetapir PET) were regressed on time between scans using linear regression for each patient, separately. Florbetapir PET values were adjusted for whole cerebellum uptake prior to the estimation of the rates. FDG and florbetapir PET rates were then adjusted for age and sex.

In the second step, patient-specific rates were regressed on baseline CSF  $A\beta_{42}$  using monotone penalized regression splines. Generalized cross-validation was used to tune the smoothing parameter and the Akaike information criterion was used to select the dimension of the basis used to represent the smooth term.<sup>30,31</sup>

Steps 1 and 2 were repeated in 500 bootstrap samples to estimate 95% confidence intervals for the association between CSF  $A\beta_{42}$  and each response using the 2.5th and 97.5th percentiles.

Permutation tests were performed to estimate the statistical significance of the association between CSF  $A\beta_{42}$  and each response. Responses were regressed on permuted values of CSF  $A\beta_{42}$  in each bootstrap sample to obtain a null distribution of  $F$  statistics.  $p$  Values were then calculated as the proportion of null  $F$  statistics that were equal to or greater than the observed  $F$  statistic estimated using the true CSF  $A\beta_{42}$  labels.

For responses with a significant association with CSF  $A\beta_{42}$ , points of initial acceleration in rate of decline with respect to  $\beta$ -amyloid pathology were estimated. These points were taken to be the moment the curves dropped 1 SE below the mean response at the highest levels of CSF  $A\beta_{42}$ . However, since the SE is sample size–dependent and the sample sizes varied with each model, we reweighted each SE to correspond to the average sample size. Standard deviations and 95% confidence intervals were estimated from the 500 bootstrap samples.

Baseline associations between demographics and CSF A $\beta$ <sub>42</sub> were assessed using Spearman correlation for age and education and the Wilcoxon rank-sum test for sex.

The association between baseline CSF A $\beta$ <sub>42</sub> and missing data were modeled using generalized mixed-effects regression for MRI and cognitive outcomes, with a binomial missing indicator for a missing visit. Similarly, logistic regression was used to assess missingness for FDG and florbetapir PET. *p* Values from permutation tests were adjusted for multiplicity using a false discovery rate correction.<sup>32</sup> All analyses were done in R v3.1.1 (www.r-project.org).

**RESULTS Cohort characteristics.** A total of 460 patients with MCI were followed longitudinally up to 8 years. A total of 420 MCI participants were included in the MRI analysis, 460 in the analysis of cognition, 193 in the FDG PET analysis, and 258 in the florbetapir PET analysis. Participants underwent MRI scans an average of 4.1 times over an average of 1.5 years (maximum 3 years). Cognitive tests were administered an average of 7.3 times over an average of 2.6 years (maximum 8 years). Participants had 2 FDG PET and florbetapir PET scans each—one at baseline and another at their 2-year visit.

Overall, baseline CSF A $\beta$ <sub>42</sub> was highly associated with age ( $\rho = -0.20$ ,  $p < 0.001$ ) and marginally associated with sex ( $p = 0.09$ ), with men having on average 8 ng/L less CSF A $\beta$ <sub>42</sub> compared with women. Years of education was not associated with baseline CSF A $\beta$ <sub>42</sub> ( $\rho = 0.02$ ,  $p = 0.63$ ). The 4 analysis groups (cognition, MRI, FDG, and florbetapir PET) were similar, with mean baseline CSF A $\beta$ <sub>42</sub> ranging from 174 to 181 ng/L, mean age ranging from 71 to 72 years, percent female ranging from 44% to 48%, mean years of education 16 for all groups, percent *APOE*  $\epsilon$ 4 carriers ranging from 43% to 49%, and mean ADAS-13 ranging from 14 to 15. All analyses were adjusted for age and sex and the cognitive analyses were also adjusted for education.

A 1 SD decrease in baseline CSF A $\beta$ <sub>42</sub> was associated with increased odds of missing FDG PET (log odds ratio [OR] =  $-0.20$ , SE = 0.10,  $p = 0.043$ ), florbetapir PET (log OR =  $-0.25$ , SE = 0.10,  $p = 0.011$ ), and marginally associated with increased odds of missing cognitive data (log OR =  $-0.09$ , SE = 0.05,  $p = 0.07$ ) and MRI data (log OR =  $-0.11$ , SE = 0.08,  $p = 0.154$ ).

**MRI.** There was significant acceleration in atrophy rates with respect to CSF A $\beta$ <sub>42</sub> in all MRI ROIs, except the cingulate gyrus. The increase in atrophy rate was estimated to start at CSF A $\beta$ <sub>42</sub> = 213 ng/L in the temporal lobe and considerably later in the rest of the lobes (with the parietal and frontal lobes accelerating at intermediate CSF A $\beta$ <sub>42</sub> levels and the occipital lobe accelerating first at very low CSF A $\beta$ <sub>42</sub> levels). Results of the overall tests of association

between CSF A $\beta$ <sub>42</sub> and MRI ROIs and also estimates of initial rate acceleration points and confidence intervals are summarized in the table. Rates of all ROIs are plotted against baseline CSF A $\beta$ <sub>42</sub>, as well as estimates of points of the initial rate acceleration, in figure 1.

**Cognitive and functional outcomes.** There was a significant acceleration in rate of decline in all 11 cognitive and functional measures across the span of baseline CSF A $\beta$ <sub>42</sub>. Global measures of cognitive decline and delayed logical memory recall were estimated to begin accelerating near CSF A $\beta$ <sub>42</sub> = 230 ng/L, with functional measures immediately following. Hypothesis tests and estimates are summarized in the table. Plots of cognitive and functional outcomes are shown in figure 2.

**FDG PET.** Significant acceleration of rates of FDG PET was observed in all 3 ROIs. A 1 SE rate increase was estimated to occur near CSF A $\beta$ <sub>42</sub> = 280 ng/L in all 3 ROIs. Estimates are summarized in the table and plots are shown in the top row of figure 3.

**Florbetapir PET.** Significant acceleration of rates of florbetapir PET was observed in all ROIs. Similar to FDG PET, a 1 SE rate increase was estimated to occur near CSF A $\beta$ <sub>42</sub> = 280 ng/L. Estimates are summarized in the table and plots are shown in the bottom row of figure 3. All imaging and cognitive points of initial acceleration and confidence intervals are shown in figure 4.

**DISCUSSION** The main findings of this analysis are (1) rates of neuronal injury, cognitive decline, and even functional decline accelerate substantially before a conventional threshold for amyloid positivity, (2) acceleration points for florbetapir PET and FDG PET were estimated to occur at approximately the same level of CSF A $\beta$ <sub>42</sub>, and (3) temporal lobe atrophy rates accelerate prior to the conventional threshold for amyloid positivity, confirming our previous report,<sup>16</sup> but they did not precede the increase in rates of cognitive and functional decline.

Rates of multiple modes of neurodegeneration, cognitive decline, and functional decline are observed to accelerate prior to the current threshold for amyloid positivity. A considerable proportion of patients with MCI would not meet inclusion criteria for a clinical trial based on the current threshold for amyloid positivity, though on average, they are experiencing cognitive and functional decline associated with pre-threshold levels of CSF A $\beta$ <sub>42</sub>. In fact, these patients would never meet criteria for any stage of preclinical AD during the course of their progression because they demonstrated clinically significant cognitive and functional impairment prior to becoming amyloid-positive.<sup>33</sup> If the efficacy of an anti-amyloid

**Table** Estimates of initial acceleration points, 95% confidence intervals, and significance of permutation tests

Outcome	Initial acceleration point (95% CI) (CSF, A $\beta_{42}$ )	Permutation test p value
<b>MRI</b>		
Temporal lobe	213 (253, 173)	<0.001
Parietal lobe	178 (239, 117)	<0.001
Frontal lobe	166 (239, 100)	0.019
Occipital lobe	136 (184, 100)	0.009
Cingulate gyrus	—	0.114
<b>Cognition/function</b>		
ADAS-13	234 (247, 221)	<0.001
Composite	231 (242, 220)	<0.001
ADAS-11	228 (243, 213)	<0.001
MMSE	228 (247, 209)	<0.001
Logical Memory II	226 (239, 213)	<0.001
FAQ	221 (257, 185)	<0.001
CDR-SB	219 (257, 181)	<0.001
Trails A	204 (262, 146)	<0.001
Trails B	200 (251, 149)	<0.001
BNT	187 (268, 106)	<0.001
dRAVLT	156 (224, 100)	0.003
<b>FDG PET</b>		
Temporal gyrus	284 (314, 206)	<0.001
Angular gyrus	279 (314, 203)	<0.001
Cingulate gyrus	271 (314, 199)	<0.001
<b>Florbetapir PET</b>		
Frontal lobe	284 (314, 254)	<0.001
Parietal lobe	278 (312, 244)	0.007
Temporal lobe	273 (307, 239)	0.005

Abbreviations: ADAS = Alzheimer's Disease Assessment Scale; BNT = Boston Naming Test; CDR-SB = Clinical Dementia Rating Sum of Boxes; CI = confidence interval; dRAVLT = delayed Rey Auditory Verbal Learning Test; FAQ = Functional Assessment Questionnaire; FDG = <sup>18</sup>F-fluorodeoxyglucose; MMSE = Mini-Mental State Examination.

treatment relies on mitigating the effect of amyloid at the initial downslope of cognitive decline, it is likely that trial inclusion criteria should be revised to include patients with substantially less  $\beta$ -amyloid pathology, especially in light of a recent report finding that those with emerging amyloid pathology (CSF A $\beta_{42}$  < 225 ng/L, but still amyloid-negative) are at increased risk of becoming amyloid-positive in the near term.<sup>34</sup>

The cognitive and atrophy rate curves are flat at high levels of CSF A $\beta_{42}$  before a distinct rate acceleration occurs. In contrast, the shape of the curves for FDG and florbetapir PET is linear without any plateau, suggesting a very early rate increase even at the least pathologic levels of CSF A $\beta_{42}$ . It is no surprise, given the high correlation between measures of  $\beta$ -amyloid in CSF and PET, that changes in

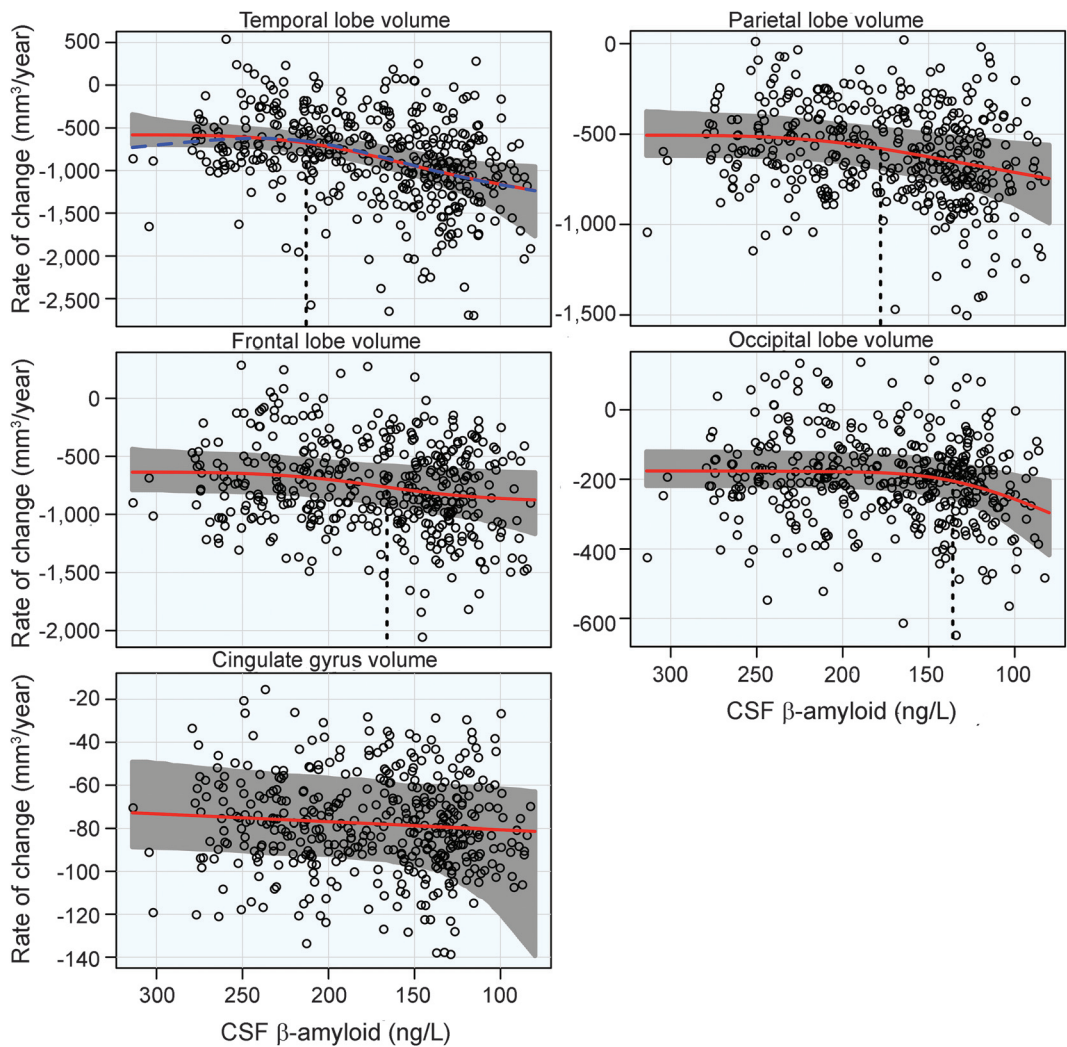
florbetapir rates and CSF A $\beta_{42}$  would occur close together. Recent reports suggest that CSF amyloid may decrease prior to an increase in amyloid deposition.<sup>34,35</sup> FDG PET and synaptic dysfunction have also been identified as early-stage processes,<sup>36</sup> although it is surprising to see changes in FDG PET, a measure of neurodegeneration, occur so closely with amyloid deposition. It is possible that there are too few observations at the highest levels of CSF A $\beta_{42}$  to estimate the plateau in the FDG PET analysis, biasing the estimates of acceleration to higher levels of CSF A $\beta_{42}$ . There is also a considerable delay between the acceleration of FDG PET rates and the acceleration of cognitive decline, as shown in figure 4. The confidence intervals for FDG PET are wide and while the time between a reduction in brain glucose metabolism and the onset of cognitive decline is unknown, it is again possible that there is an upward bias for the FDG PET estimates of acceleration.

The third result of our analysis is the unexpected timing of the acceleration of atrophy rates compared to cognition. However, given the association between FDG PET and cognition, it makes sense that increased rates of cognitive decline would immediately follow worsening synaptic dysfunction, prior to the actual physical degeneration and loss of gray matter. It is also possible that the age adjustment may affect the estimates for atrophy acceleration more than other outcomes, given the high degree of association between aging and atrophy. The estimate of the point of initial acceleration of rate of temporal lobe atrophy (CSF A $\beta_{42}$  = 213 ng/L) is similar to estimates previously reported in a different cohort.<sup>16</sup> However, a plateau in atrophy at low levels of CSF A $\beta_{42}$  was not replicated here, possibly due to a less progressed cohort studied here.

The results of this analysis provide some evidence for the ordering of markers for neurodegeneration and cognitive decline with respect to CSF A $\beta_{42}$ , but not formal statistical tests. Figure 4 shows wide confidence intervals for all markers, with the exception of the global cognitive measures and delayed logical memory, which are surprisingly narrow. We opted to include all available data for each outcome in order to get the most precise estimates of rate changes; however, this resulted in varying sample sizes across outcomes. Additional studies will be required to make formal conclusions about the specifics of the order; however, it appears that the rates of nearly all the biomarkers in this study begin to increase prior to what is considered the threshold for amyloid positivity.

These analyses do not provide evidence that amyloid plays a causal role in the increase of neurodegeneration and cognitive decline. It is possible that

**Figure 1** MRI rates of change

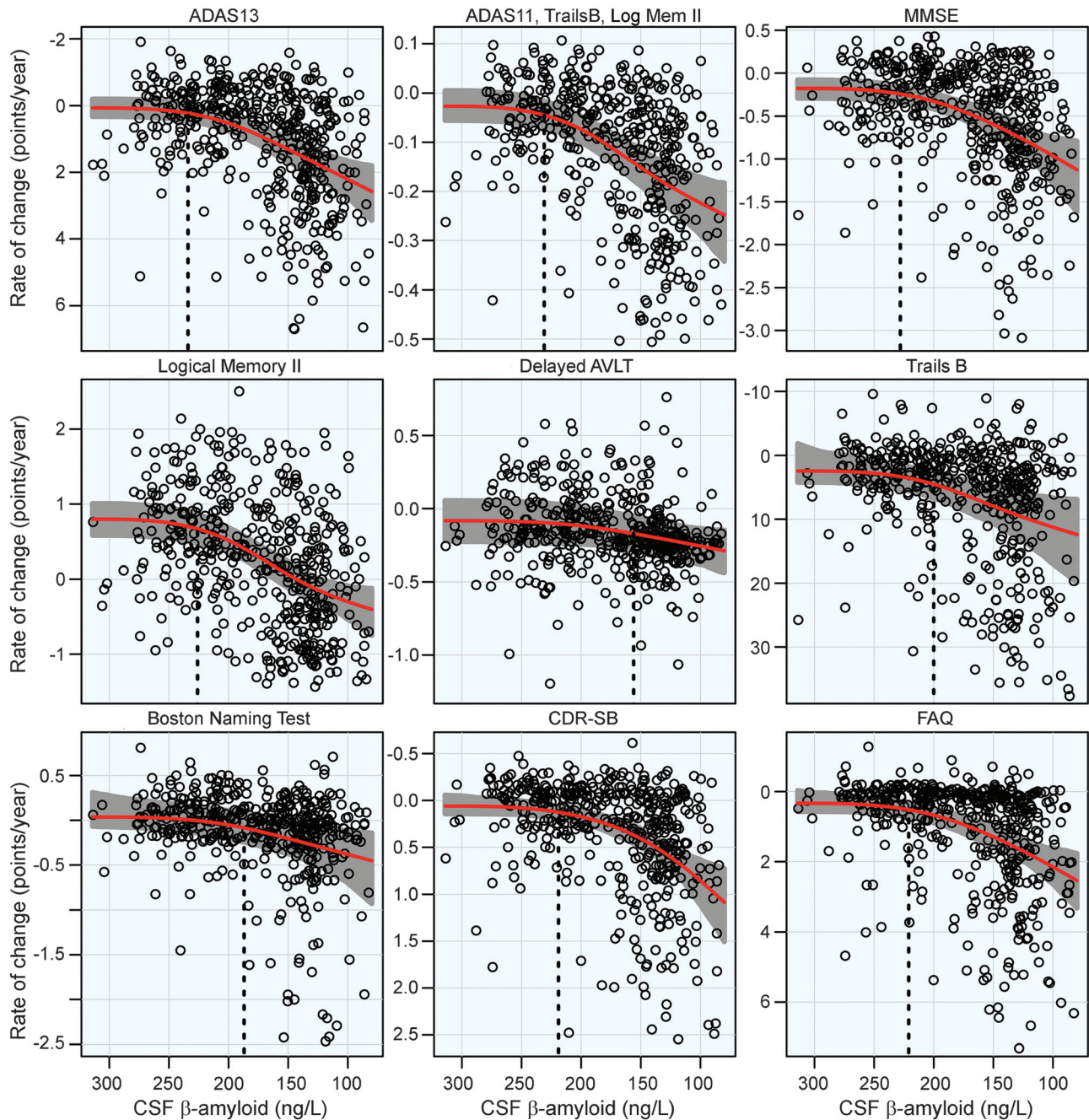


Annual rates of change of MRI regions are plotted against baseline CSF  $A\beta_{42}$ . Atrophy rates increase from top to bottom and  $\beta$ -amyloid pathology increases from left to right. Estimated curves are in red with 95% confidence intervals shaded in gray. The dashed blue line in the plot of the temporal lobe is the estimated curve without the monotonicity restriction, for comparison. The vertical dashed line in black is the estimate of the initial acceleration point, if it exists.

neuronal injury and cognitive decline are due to increased amyloid deposition; however, it is also possible that amyloid deposition is a downstream effect of other unobserved factors. It is likely that the amyloid burden required to elicit increased neuronal injury varies greatly across patients in this cohort. Some may be susceptible to minimal levels of amyloid deposition, while others may only show signs of neurodegeneration after prolonged amyloid deposition. Or some patients may exhibit substantial neurodegeneration prior to even minimal amyloid deposition. Our models are a simplified version of the relationships among biomarkers and cognition. A more complex model, one that adjusted the association between CSF  $A\beta_{42}$  and cognition for cortical atrophy, for example, may yield different results with different estimates of points of initial rate

acceleration. Additional risk factors not considered in this analysis are also likely at play, including cerebrovascular disease, and other proteinopathies including  $\alpha$ -synuclein and TDP-43.<sup>37,38</sup> Another consideration is the heterogeneity of the MCI population. While we focus on estimates averaged over the entire cohort, it is likely that some patients' rates begin to increase after the conventional threshold for amyloid positivity. Floor effects of some measures may also bias estimates of acceleration. For example, the estimate of acceleration observed in dRAVLT, a measure thought to decline early, is noticeably later than other measures of cognition, especially measures including delayed memory recall. The late estimate of acceleration is likely due to many MCI patients already scoring near the floor of the measure with no room to decline.

**Figure 2** Cognitive and functional rates of change

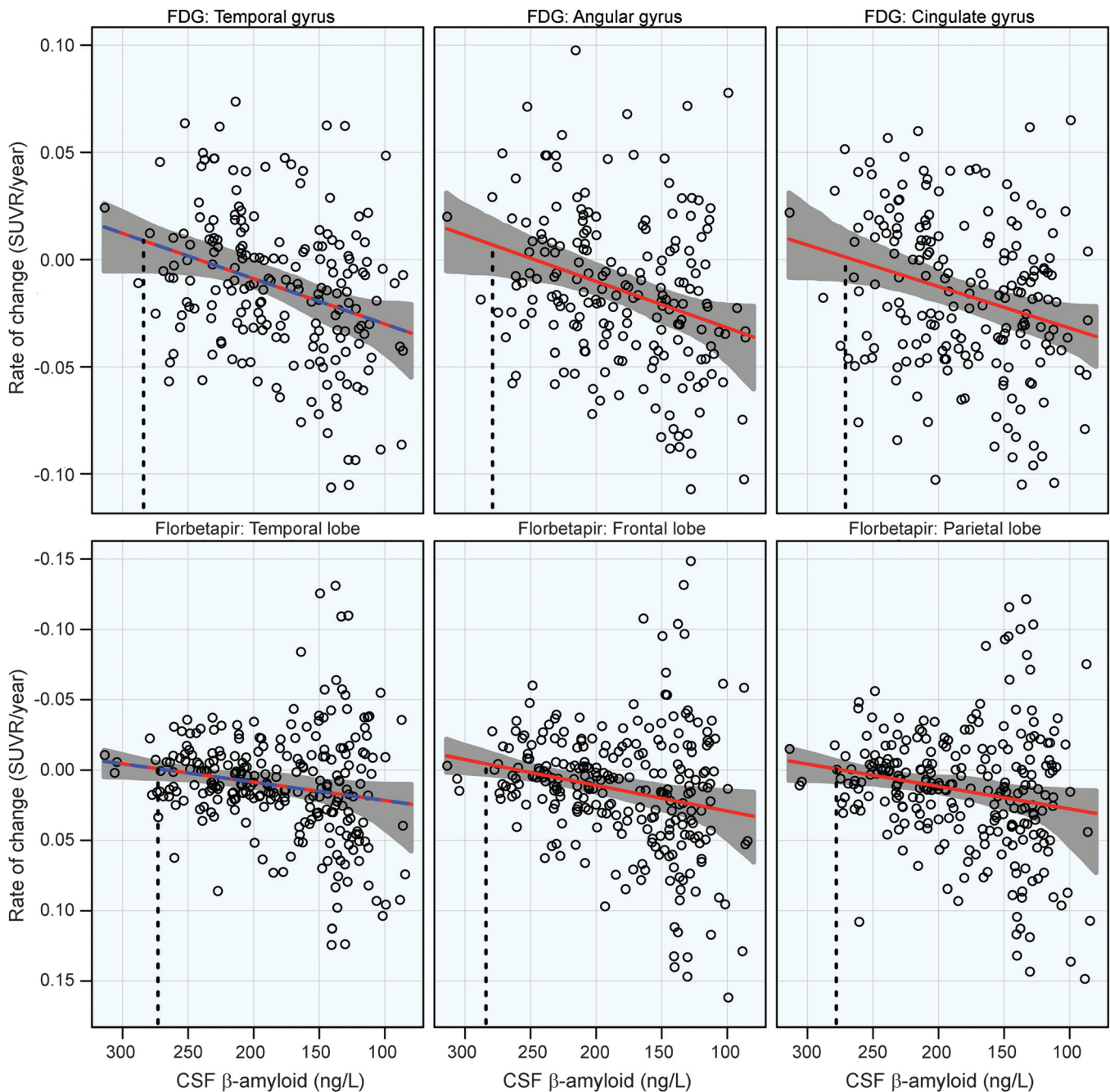


Annual rates of change for cognitive and functional measures are plotted against baseline CSF A $\beta_{42}$ . Rates of cognition or function worsen from top to bottom and  $\beta$ -amyloid pathology increases from left to right. Estimated curves are in red with 95% confidence intervals shaded in gray. The vertical dashed line in black is the estimate of the initial acceleration point. ADAS = Alzheimer's Disease Assessment Scale; AVLT = Auditory Verbal Learning Test; CDR-SB = Clinical Dementia Rating Sum of Boxes; FAQ = Functional Assessment Questionnaire; MMSE = Mini-Mental State Examination.

While this study only examined patients with MCI, understanding the sequence of biomarker change in a cognitively normal population will be important for the design of clinical trials in a presymptomatic population. A large population of amyloid-positive cognitively normal people resist the cognitive decline seen in their MCI-affected peers, and a large proportion has done it with a considerably larger amyloid burden, given the low levels of amyloid shown to be associated

with decline in this study. The ability of some to tolerate large amounts of amyloid, while others demonstrate decline much earlier in the process of amyloid accumulation, remains a gray area in understanding the progression of AD and an obstacle for the design of clinical trials. By making amyloid thresholds more liberal, there may be some loss in specificity; however, this loss may be worth the gains made by treating a less progressed population.

**Figure 3**  $^{18}\text{F}$ -fluorodeoxyglucose (FDG) and florbetapir PET rates of change



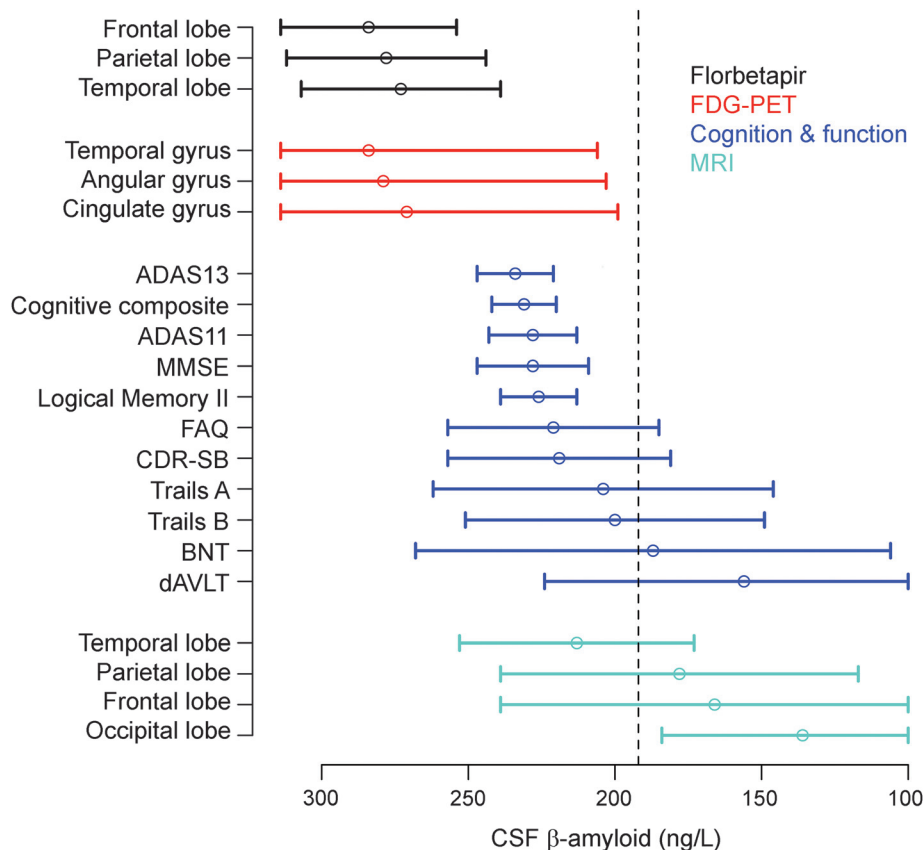
Annual rates of change for FDG PET (top row) and florbetapir (bottom row) are plotted against baseline CSF  $\text{A}\beta_{42}$ . Rates worsen from top to bottom and  $\beta$ -amyloid pathology increases from left to right. Estimated curves are in red with 95% confidence intervals shaded in gray. The dashed blue line in the plot of the temporal lobe is the estimated curve without the monotonicity restriction, for comparison. The vertical dashed line in black is the estimate of the initial acceleration point. SUVR = standardized uptake value ratio.

Even with an optimal amyloid threshold, considerable variability will remain regarding the association between  $\text{A}\beta$  pathology and cognition in elders, given that a similar degree of  $\text{A}\beta$  pathology may be seen in people who are cognitively normal, slightly impaired, or with full dementia. This variability highlights the importance of assessing other screening characteristics besides  $\text{A}\beta$  status, including specific markers for neurodegeneration such as FDG

PET, tau pathology, and gray matter atrophy, when selecting preclinical populations for trial enrichment. It is possible that a threshold for the risk of progression should not be based on  $\text{A}\beta$  or neurodegeneration alone, but rather inclusion into a trial requires some interdependent minimal level of both types of pathology.

Future clinical trials in early AD might consider revising the criteria regarding  $\beta$ -amyloid thresholds

**Figure 4** Acceleration point estimates and 95% confidence intervals



Estimates of the initial acceleration points and 95% confidence intervals for all outcomes are plotted against baseline CSF A $\beta_{42}$ .  $\beta$ -Amyloid pathology increases from left to right. The dashed black line is the conventional threshold for amyloid positivity (192 ng/L). ADAS = Alzheimer's Disease Assessment Scale; BNT = Boston Naming Test; CDR-SB = Clinical Dementia Rating Sum of Boxes; dRAVLT = delayed Rey Auditory Verbal Learning Test; FAQ = Functional Assessment Questionnaire; FDG =  $^{18}$ F-fluorodeoxyglucose; MMSE = Mini-Mental State Examination.

to include the range of amyloid associated with the first signs of accelerating rates of decline.

### AUTHOR CONTRIBUTIONS

P.S. Insel drafted and revised the manuscript for content, contributed to the study design, and analyzed and interpreted the data. Dr. Mattsson revised the manuscript for content, contributed to the study design, and interpreted the data. Dr. Mackin revised the manuscript for content and interpreted the data. Dr. Schöll revised the manuscript for content. Dr. Nosheny revised the manuscript for content. Dr. Tosun revised the manuscript for content. Dr. Donohue revised the manuscript for content, contributed to the study design, and interpreted the data. Dr. Aisen revised the manuscript for content. Dr. Jagust revised the manuscript for content. Dr. Weiner revised the manuscript for content.

### STUDY FUNDING

Data collection and sharing for this project was funded by the Alzheimer's Disease Neuroimaging Initiative (ADNI) (NIH grant U01 AG024904). ADNI is funded by the National Institute on Aging, the National Institute of Biomedical Imaging and Bioengineering, and through contributions from the following: Alzheimer's Association; Alzheimer's Drug Discovery Foundation; BioClinica, Inc.; Biogen Idec Inc.; Bristol-Myers Squibb Company; Eisai Inc.; Elan Pharmaceuticals, Inc.; Eli Lilly and Company; F. Hoffmann-La Roche Ltd. and its affiliated company Genentech, Inc.; GE Healthcare; Innogenetics, N.V.; IXICO Ltd.; Janssen Alzheimer Immunotherapy Research & Development, LLC; Johnson & Johnson Pharmaceutical Research & Development LLC; Medpace, Inc.; Merck & Co., Inc.; Meso Scale Diagnostics,

LLC; NeuroRx Research; Novartis Pharmaceuticals Corporation; Pfizer Inc.; Piramal Imaging; Servier; Synarc Inc.; and Takeda Pharmaceutical Company. The Canadian Institutes of Health Research is providing funds to support ADNI clinical sites in Canada. Private sector contributions are facilitated by the Foundation for the NIH ([www.fnih.org](http://www.fnih.org)). The grantee organization is the Northern California Institute for Research and Education, and the study is coordinated by the Alzheimer's Disease Cooperative Study at the University of California, San Diego. ADNI data are disseminated by the Laboratory for Neuroimaging at the University of Southern California. This research was also supported by NIH grants P30 AG010129 and K01 AG030514.

### DISCLOSURE

P. Insel and N. Mattsson report no disclosures relevant to the manuscript. R. Mackin has financial support from NIMH R01 0977669 and NIMH K08 MH081065. M. Schöll, R. Nosheny, and D. Tosun report no disclosures relevant to the manuscript. M. Donohue was a consultant for Bristol-Myers Squibb. P. Aisen serves on a scientific advisory board for NeuroPhage; has served as a consultant to Elan, Wyeth, Eisai, Schering-Plough, Bristol-Myers Squibb, Eli Lilly and Company, NeuroPhage, Merck, Roche, Amgen, Genentech, Abbott, Pfizer, Novartis, Bayer, Astellas, Dainippon, Biomearin, Solvay, Otsuka, Daiichi, AstraZeneca, Janssen, Medivation, Ichor, Toyama, Lundbeck, Biogen Idec, iPerian, Probiobdrug, Somaxon, Biotie, Cardeus, Anavex, Kyowa Hakkō Kirin Pharma, and Medtronic; and receives research support from Eli Lilly and Baxter and the NIH (NIA U01-AG10483 [PI], NIA U01-AG024904 [Coordinating Center Director], NIA R01-AG030048 [PI], and R01-AG16381 [Co-I]). W. Jagust reports no disclosures relevant to the manuscript. M. Weiner has been on scientific advisory boards for Pfizer and



BOLT International; has been consultant for Pfizer Inc., Janssen, KLIJ Associates, Easton Associates, Harvard University, inThought, INC Research, Inc., University of California, Los Angeles, Alzheimer's Drug Discovery Foundation, and Sanofi-Aventis Group; has received funding for travel from Pfizer, ADPD meeting, Paul Sabatier University, Novartis, Tohoku University, MCI Group, France, Travel eDreams, Inc., Neuroscience School of Advanced Studies (NSAS), Danone Trading, BV, and CTAD ANT Congress; serves as an associated editor of *Alzheimer's & Dementia*; has received honoraria from Pfizer, Tohoku University, and Danone Trading BV; has research support from Merck, Avid, DOD and VA; and has stock options in Synarc and Elan. Go to Neurology.org for full disclosures.

Received October 7, 2015. Accepted in final form February 9, 2016.

## REFERENCES

- Donohue MC, Jacqmin-Gadda H, Le Goff M, et al. Estimating long-term multivariate progression from short-term data. *Alzheimers Dement* 2014;10:S400–S410.
- Jack CR, Knopman DS, Jagust WJ, et al. Hypothetical model of dynamic biomarkers of the Alzheimer's pathological cascade. *Lancet Neurol* 2010;9:119–128.
- Bateman RJ, Xiong C, Benzinger TL, et al. Clinical and biomarker changes in dominantly inherited Alzheimer's disease. *N Engl J Med* 2012;367:795–804.
- Jack CR, Knopman DS, Jagust WJ, et al. Tracking pathophysiological processes in Alzheimer's disease: an updated hypothetical model of dynamic biomarkers. *Lancet Neurol* 2013;12:207–216.
- Hyman BT. Amyloid-dependent and amyloid-independent stages of Alzheimer disease. *Arch Neurol* 2011;68:1062–1064.
- Doody RS, Thomas RG, Farlow M, et al. Phase 3 trials of solanezumab for mild-to-moderate Alzheimer's disease. *N Engl J Med* 2014;370:311–321.
- Sperling RA, Jack CR, Aisen PS. Testing the right target and right drug at the right stage. *Sci Translational Med* 2011;3:111cm33.
- Karran E, Hardy J. Anti-amyloid therapy for Alzheimer's disease: are we on the right road?. *N Engl J Med* 2014;370:377–378.
- Sperling RA, Rentz DM, Johnson KA, et al. The A4 study: stopping AD before symptoms begin?. *Sci Transl Med* 2014;6:228fs13.
- Shaw LM, Vanderstichele H, Knapik-Czajka M, et al. Cerebrospinal fluid biomarker signature in Alzheimer's disease neuroimaging initiative subjects. *Ann Neurol* 2009;65:403–413.
- Landau SM, Mintun MA, Joshi AD, et al. Amyloid deposition, hypometabolism, and longitudinal cognitive decline. *Ann Neurol* 2012;72:578–586.
- Jack CR, Vemuri P, Wiste HJ, et al. Evidence for ordering of Alzheimer disease biomarkers. *Arch Neurol* 2011;68:1526–1535.
- Villeneuve S, Rabinovici GD, Cohn-Sheehy BI, et al. Existing Pittsburgh compound B positron emission tomography thresholds are too high: statistical and pathological evaluation. *Brain* 2015;138:2020–2033.
- Reiman EM, Quiroz YT, Fleisher AS, et al. Brain imaging and fluid biomarker analysis in young adults at genetic risk for autosomal dominant Alzheimer's disease in the presenilin 1 E280A kindred: a case-control study. *Lancet Neurol* 2012;11:1048–1056.
- Filippini N, MacIntosh BJ, Hough MG, et al. Distinct patterns of brain activity in young carriers of the APOE-ε4 allele. *Proc Natl Acad Sci USA* 2009;106:7209–7214.
- Insel PS, Mattsson N, Donohue MC, et al. The transitional association between β-amyloid pathology and regional brain atrophy. *Alzheimers Dement* 2015;11:1171–1179.
- Olsson A, Vanderstichele H, Andreasen N, et al. Simultaneous measurement of beta-amyloid(1-42), total tau, and phosphorylated tau (Thr181) in cerebrospinal fluid by the xMAP technology. *Clin Chem* 2005;51:336–345.
- Jack CR, Bernstein MA, Fox NC, et al. The Alzheimer's Disease Neuroimaging Initiative (ADNI): MRI methods. *J Magn Reson Imaging* 2008;27:685–691.
- Fischl B, Salat DH, Busa E, et al. Whole brain segmentation: automated labeling of neuroanatomical structures in the human brain. *Neuron* 2002;33:341–355.
- Jagust WJ, Bandy D, Chen K, Foster NL, Landau SM, Mathis CA. The Alzheimer's Disease Neuroimaging Initiative positron emission tomography core. *Alzheimers Dement* 2010;6:221–229.
- Landau SM, Harvey D, Madison CM, et al. Associations between cognitive, functional, and FDG-PET measures of decline in AD and MCI. *Neurobiol Aging* 2011;32:1207–1218.
- Reitan R. Validity of the Trail-Making test as an indication of organic brain damage. *Percept Mot Skills* 1958;8:271–276.
- Wechsler DA. Wechsler Adult Intelligence Scale–Revised. New York: Psychological Corporation; 1987.
- Kaplan EF, Goodglass H, Weintraub S. The Boston Naming Test, 2nd ed. Philadelphia: Lea & Febiger; 1982.
- Rey A. l'Examen Clinique En Psychologie. Paris: Presses Universitaires de France; 1964.
- Rosen WG, Mohs RC, Davis KL. A new rating scale for Alzheimer's disease. *Am J Psychiatry* 1984;141:1356–1364.
- Pfeffer RI, Kurosaki TT, Harrah CH, Chance JM, Filos S. Measurement of functional activities of older adults in the community. *J Gerontol* 1982;37:323–329.
- Morris JC. Clinical dementia rating. *Neurology* 1993;43:2412–2414.
- Insel PS, Mattsson N, Mackin RS, et al. Biomarkers and cognitive endpoints to optimize trials in Alzheimer's disease. *Ann Clin Transl Neurol* 2015;2:534–547.
- Wood SN. Generalized Additive Models: An Introduction with R. Boca Raton, FL: Chapman and Hall/CRC Press; 2006.
- Wood SN. Monotonic smoothing splines fitted by cross validation. *SIAM J Sci Comput* 1994;15:1126–1133.
- Benjamini Y, Hochberg Y. Controlling the false discovery rate: a practical and powerful approach to multiple testing. *J R Stat Soc Ser B* 1995;57:289–300.
- Sperling RA, Aisen PS, Beckett LA, et al. Toward defining the preclinical stages of Alzheimer's disease: recommendations from the National Institute on Aging-Alzheimer's Association workgroups on diagnostic guidelines for Alzheimer's disease. *Alzheimers Dement* 2011;7:280–292.
- Mattsson N, Insel PS, Donohue M, et al. Predicting reduction of cerebrospinal fluid β-amyloid 42 in cognitively healthy controls. *JAMA Neurol* 2015;72:554–560.
- Mattsson N, Insel PS, Donohue M, et al. Independent information from cerebrospinal fluid amyloid-β and florbetapir imaging in Alzheimer's disease. *Brain* 2015;138:772–783.
- Reiman EM, Caselli RJ, Chen K, Alexander GE, Bandy D, Frost J. Declining brain activity in cognitively

- normal apolipoprotein E  $\epsilon 4$  heterozygotes: a foundation for using positron emission tomography to efficiently test treatments to prevent Alzheimer's disease. *Proc Natl Acad Sci* 2001;98:3334–3339.
37. Mackin RS, Insel P, Zhang J, et al. Cerebrospinal fluid  $\alpha$ -synuclein and Lewy body-like symptoms in normal controls, mild cognitive impairment, and Alzheimer's disease. *J Alzheimers Dis* 2015;43:1007–1016.
38. Keage HA, Hunter S, Matthews FE, et al. TDP-43 pathology in the population: prevalence and associations with Dementia and age. *J Alzheimers Dis* 2014;42:641–650.

## Subspecialty Alerts by E-mail!

Customize your online journal experience by signing up for e-mail alerts related to your subspecialty or area of interest. Access this free service by visiting [Neurology.org/site/subscriptions/etoc.xhtml](http://Neurology.org/site/subscriptions/etoc.xhtml) or click on the “E-mail Alerts” link on the home page. An extensive list of subspecialties, methods, and study design choices will be available for you to choose from—allowing you priority alerts to cutting-edge research in your field!

## Get Your Front Row Seat to the Premier Event on Sports Concussion

The world's leading experts on sports concussion are once again hosting the year's premier event on sports concussion. The American Academy of Neurology's 2016 Sports Concussion Conference, set for July 8 through 10 in Chicago, features a concussion boot camp and is poised to be *the go-to* meeting for all disciplines involved in the prevention, diagnosis, and treatment of professional, collegiate, and high school sports concussion, including neurologists, athletic trainers, and other medical professionals. Early registration discounts end June 14, so visit [AAN.com/view/ConcussionConference](http://AAN.com/view/ConcussionConference) to secure your spot—and savings—today!

## Neurology® Genetics Call For Papers



*Neurology: Genetics* is an open access, online only journal that provides neurologists with outstanding original contributions that elucidate the role of genetic and epigenetic variation in diseases and biological traits of the central and peripheral nervous system. We welcome all submissions. For more information on how to submit, visit <http://www.neurology.org/site/gen/gen2.xhtml>.